

4605 (errors:5) words

File: main.tex  
Encoding: utf8  
Sum count: 4605  
Words in text: 3740  
Words in headers: 47  
Words outside text (captions, etc.): 748  
Number of headers: 18  
Number of floats/tables/figures: 11  
Number of math inlines: 58  
Number of math displayed: 12  
Subcounts:  
text+headers+captions (#headers/#floats/#inlines/#displayed)  
26+8+0 (1/0/0/0) \_top\_  
304+1+0 (1/0/0/0) Section: Abstract  
925+1+81 (1/1/1/0) Section: Introduction  
37+1+12 (1/1/0/0) Section: Methods} \label{methods  
343+6+0 (4/0/30/8) Subsection: Constraints  
72+1+0 (1/0/5/1) Subsection: Objective  
331+2+0 (1/0/0/0) Subsection: Metabolic phenotypes} \label{phenotype\_methods  
689+12+37 (3/1/17/3) Subsection: E. coli-Pseudomonas competitive community  
0+3+0 (1/0/0/0) Section: Results and Discussion  
165+8+163 (1/1/0/0) Subsection: New data fitting method for iterative experimental design  
187+2+0 (1/0/1/0) Subsection: Simulation insights  
265+1+455 (1/7/4/0) Subsection: Validation  
396+1+0 (1/0/0/0) Section: Conclusion

File: output.bbl  
Encoding: utf8  
Sum count: 0  
Words in text: 0  
Words in headers: 0  
Words outside text (captions, etc.): 0  
Number of headers: 0  
Number of floats/tables/figures: 0  
Number of math inlines: 0  
Number of math displayed: 0

Total  
Sum count: 4605  
Words in text: 3740  
Words in headers: 47  
Words outside text (captions, etc.): 748  
Number of headers: 18  
Number of floats/tables/figures: 11  
Number of math inlines: 58  
Number of math displayed: 12  
Files: 2  
Subcounts:  
text+headers+captions (#headers/#floats/#inlines/#displayed)  
3740+47+748 (18/11/58/12) File(s) total: main.tex  
0+0+0 (0/0/0/0) File(s) total: output.bbl

(errors:5)

# A microbial community growth model for phenotypic investigations

Andrew P. Freiburger<sup>1</sup>, Jeffrey A. Dewey<sup>1</sup>, Fatima Foflonker<sup>1</sup>, Gyorgy Babnigg<sup>2</sup>, Dionysios A. Antonopoulos<sup>2</sup>, and Christopher Henry<sup>1\*</sup>

<sup>1</sup>Argonne National Laboratory, Computing, Environment, and Life Sciences Division, Lemont, IL 60148 USA

<sup>2</sup>Argonne National Laboratory, Biosciences Division, Lemont, IL 60148 USA  
\*e-mail: cshenry@anl.gov

December 6, 2022

## 1 Abstract

Microbial communities are increasingly recognized as decisive agents in animal health, agricultural productivity, industrial operations, and ecological systems. The plethora of chemical interactions in these complex communities, however, can complicate or evade experimental studies, which hinders basic understanding and limits efforts to rationally design communities for applications in the aforementioned fields. Numerous computational approaches have been proposed to deduce these metabolic interactions – notably including flux balance analysis (FBA) and systems of ordinary differential equations (ODEs) – yet, these methods either fail to capture dynamic phenotypic abundances of community members or are insufficiently flexible to accommodate the array of data types and structures that may be acquired experimentally.

We therefore developed a dynamic model (CommPhitting) that deduces phenotype abundances and growth kinetics for each community member, concurrent with metabolic concentrations, by coupling flux profiles for each phenotype with experimental growth and -omics data of the community. These data are parameterized, as variables and coefficients in linear constraints for biological processes, that is globally optimized to determine the species and phenotype biomasses, phenotype growth kinetics, and metabolite concentrations at each time point that best recapitulate the data. We exemplify CommPhitting with batch growth, metabolomics, and BIOLOG data of an idealized yet unstudied two-member community of model physiologic and environmental organisms (*Escherichia coli* and *Pseudomonas fluorescens*) that exhibits cross-feeding in maltose media. Simulations of this community resolved kinetics parameters and phenotype proportions which would be difficult to experimentally ascertain, yet are important for understanding community responses to environmental perturbations and therefore engineering applications: e.g. for bioproduction. We believe that CommPhitting – which is generalized for a diversity of data types and formats, and is further available and amply documented as Python API in the ModelSEEDpy library – will augment basic understanding of microbial communities and will accelerate the engineering of synthetic communities diverse applications in medicine, agriculture, industry, and ecology.

## 2 Introduction

Microbial communities are ubiquitous on Earth [1], and serve fundamental roles as eukaryotic symbionts [2, 3, 4] and pathogens [5, 6], industrial assets [7] and antagonists [8], and ecological agents of biogeochemical cycling [9, 10, 11]. Microbial communities are therefore essential to understand in fields as diverse as medicine [12, 13] and climatology [14, 15, 16]. The assemblage of microbes into a community, while inviting intimate competition [17], offers a few advantages that make it biologically favorable in most conditions. Firstly, diversification in a) genetic potential, b) biochemical vulnerabilities [18], and c) metabolic machinery [19, 20, 21] allows community members to grow in otherwise inhospitable conditions, e.g. nutrient-poor or toxic environments, by relying on well-adapted members. Secondly, specialization among the members enables the community to achieve more efficient production of vital nutrients [22] and greater growth rates [23] than is possible by isolated, autonomous, members. These cooperative interactions, which justify community assemblage, are both predicated upon a metabolic economy of cross-feeding, where thriving members support struggling members and auxotrophic specialists exchange products to mutually satisfy nutritional requirements [24, 25]. Metabolic cross-feeding is therefore essential to understand and eventually engineer communities for desirable properties [26], such as bioproduction

applications that exceed the capabilities of monocultures [7] or sustainable biotechnology by coupling phototrophs and heterotrophs [27].

Metabolic cross-feeding (or syntrophy), despite being the crux of microbial communities, is difficult to experimentally measure. One reason is that some metabolites do not detectably accumulate in the media, which obviates all but a few experimental methods, such as fluxomics isotope labeling [28]. A second difficulty, which proves to be more formidable, is that the combinatorial quantity of cross-feeding exchanges creates an untenable multitude of experiments to resolve all possible interactions in natural communities. These challenges are further compounded by the numerous metabolic phenotypes of each member that dynamically respond, even in clonal monocultures [29], to environmental conditions. Phenotype variability is necessary to understand community dynamics, and particularly to engineer members for production or exclusion, but this analysis adds another experimental dimension to an already challenging and expensive series of measurements.

Computational biology offers a few tools to resolve the metabolic nuances of microbial communities. Flux Balance Analysis (FBA) [30], for example, is a prominent framework for simulating cellular metabolism and has been applied in numerous software tools that seek to resolve metabolic interactions within microbial communities: e.g. BacArena [31],  $\mu$ bialSim [32], dOptCom [33], SMETANA [34], CASINO [2], and MICOM [35], to name a few. FBA is attractive as a simple method for simulating metabolism that can operate without or, optionally, with experimental -omics data types [36] such as metabolomics [37, 38], proteomics [39], transcriptomics [40, 41, 42], or multi-omics [43] data. The under-determined linear problem of FBA, however, often lessens the precision and consistency of predictions and FBA moreover cannot natively capture phenotype variability within a given species metabolic model. Machine-learning algorithms [44, 45], in contrast, offer more exploratory flexibility for phenotype abundances from experimental data, but often lack the mechanisms that cultivate basic understanding and design principles. Differential equation models offers precise mechanistic explanations for predictions but has the converse problem [46] of frequently being stiff and insufficiently unbiased to flexibly explore unparameterized spaces. Fitting models, by contrast, as a final popular tool of computational biology, can be flexible enough to acquiesce new information from experimental data [47, 48, 49] while maintaining sufficient mechanistic resolution for basic understanding. Fitting methods have been accordingly applied to deduce kinetics coefficients [50] or phenotype expression [40] from experimental -omics data, but these methods do not convey time-resolved phenotype abundances within context of other experimental dimensions, such as metabolic concentration, that cultivate comprehensive understanding.

We therefore developed a global fitting model (CommPhitting) that deduces time-resolved information from experimental data: such as a) biomass of each community member and member phenotype; b) total concentrations of all metabolites that are used by the phenotypes; c) growth kinetics for each member phenotype; and d) conversion factors from each experimental signal to biomass that may accelerate the interpretation of future experiments. CommPhitting is a multi-species dynamic model of the community member phenotypes [? ], where the phenotype flux profiles are rigorously defined through a sequence of FBA simulations – 1) a minimal growth is constrained (to prevent singularities); 2) carbonaceous non-phenotype consumption is minimized (to isolate the phenotype); 3) consumption of the phenotype source is minimized (to maximize the biomass yield); 4) optionally, specified phenotype excretions are maximized (to mirror experimental phenotypes); and 5) total flux is minimized (to find the most parsimonious flux profile) – that extends previously defined methods [40]. CommPhitting is generalized for various data types into a linear problem [51] that solves simultaneously to ensure that a global optimum is determined [52], and is concisely coded to execute within a minute on a personal computer.

We exemplify CommPhitting with an idealized 2-member community of model organisms (*Escherichia coli* and *Pseudomonas fluorescens*), who exhibit complementary carbon preferences [53] but have not been investigated as a coculture. This benchtop community [54] demonstrated pivotal cross-feeding with acetate excreta from *E. coli* that was able to cultivate growth of *P. fluorescens* in a non-viable media of maltose (Figure 1). CommPhitting fit the experimental growth data remarkably well, and the predictions of phenotype abundances and metabolic concentrations were validated with transcriptomics data from the NCBI GEO database [55] and in-house metabolomics measurements of our community, respectively. We further simulated BIOLOG data from this community, which revealed growth kinetics of this community for each condition and may have broad utility for predicting community behaviors in a variety of conditions. We anticipate using the knowledge from these simulations to guide the engineering of *E. coli* for community bioproduction. CommPhitting is available as an open-source Python module in the ModelSEEDpy and is operable with the KBase [56] ecosystem. We believe that this light-weight yet robust fitting model will illuminate nuances of community interactions and cultivate rational design of microbial communities for myriad fundamental and industrial applications.

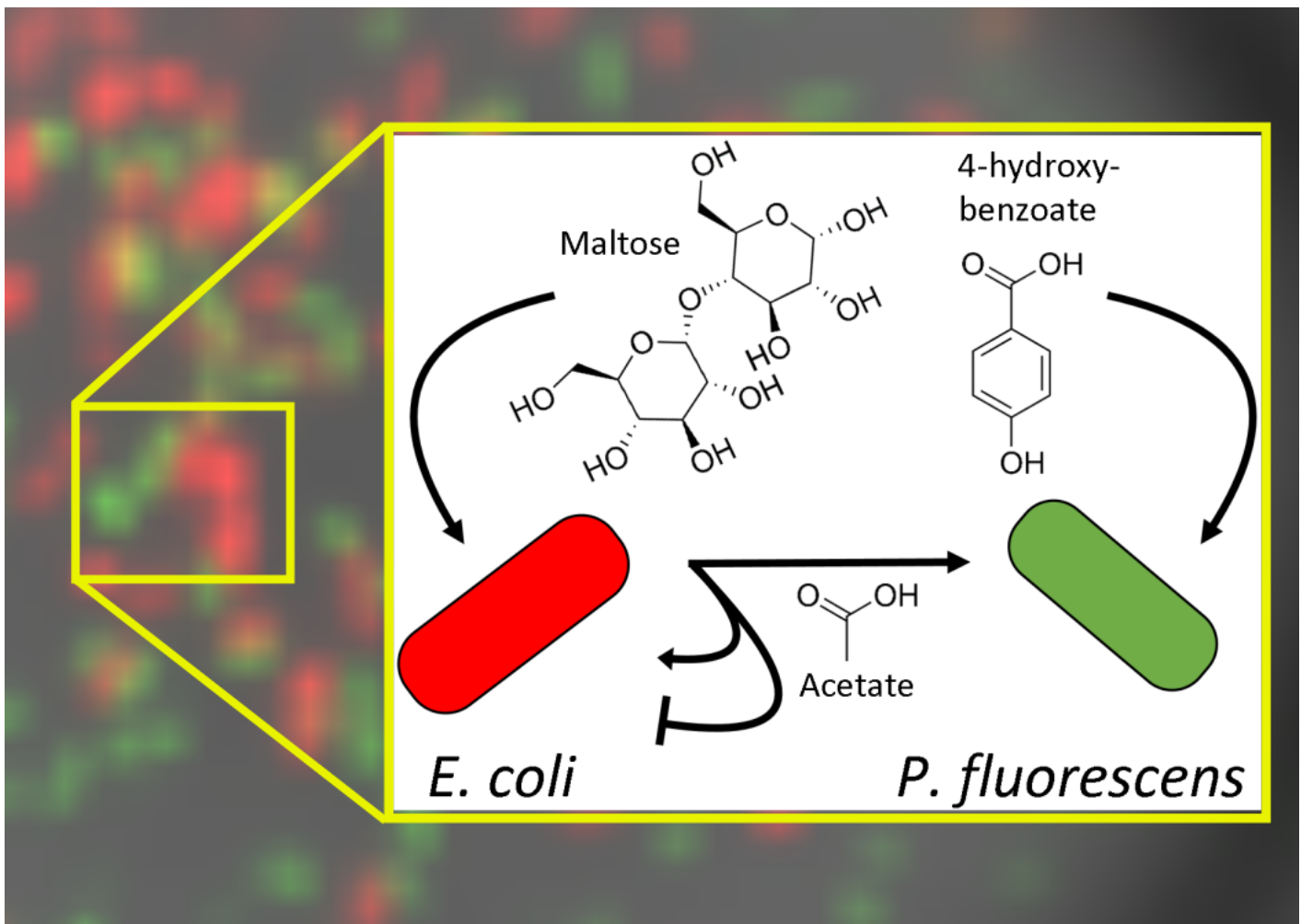


Figure 1: The primary metabolic exchanges that were experimentally elucidated and computationally modeled. The acetate byproduct of *E. coli* is the pivotal exchange of metabolic interest, where this source subsists *P. fluorescens*'s existence in maltose and exhibits interesting dual effects upon *E. coli* as both a secondary carbon source and a growth inhibitor. Additional experiments revealed that *E. coli* is reluctant to grow in pure acetate and most often fails to grow at all, particularly when in cocultures with *P. fluorescens*.

### 3 Methods

CommPhitting defines numerous parameters and variables in Table 1, linear constraints, and an objective function to capture a microbial community over time into a linear problem. These aspects of the linear problem are elaborated in the following sub-sections.

#### 3.1 Constraints

The following linear constraints of CommPhitting categorically represent aspects of community biology.

##### 3.1.1 Biomass abundances

The experimental biomass abundance ( $EB_{s,t,j}$ ), over all experimental trials  $j \in J$  and time points  $t \in T$ , is determined by converting the experimental signal ( $E_{s,t,j}$ ) via a unique coefficient ( $EC_s$ ) for each member  $s \in S$

$$E_{s,t,j} * EC_s = EB_{s,t,j} . \quad (1)$$

The variance ( $EV_{s,t,j}$ ) between the converted experimental biomass and the predicted biomass abundance  $b_{k,t,j}$  is determined for each phenotype  $k \in K$

$$EB_{s,t,j} - \sum_{s,k}^{S,K} (es_s * b_{k,t,j}) = EV_{s,t,j} , \quad (2)$$

where only the phenotypes of each respective species are considered with the binary  $es_s$  variable.

##### 3.1.2 Phenotype transitions

The biomass change over time is calculated for non-stationary (growing) phenotypes

$$b_{t,j,k} + \frac{\Delta t}{2} (g_{t,j,k} + g_{t+1,j,k}) + cvf_{t,j,k} - cvt_{t,j,k} = b_{t+1,j,k} . \quad (3)$$

The constraint consists of terms for the current biomass ( $b_{k,t,j}$ ), the biomass growth rate  $g_{k,t,j}$  as the biomass derivative ( $\frac{\Delta \text{biomass}}{\Delta t}$ ), the biomass in the next timestep ( $b_{k,t+1,j}$ ), and the net transition of biomass to non-stationary metabolic phenotypes  $cvf_{k,t,j} - cvt_{k,t,j}$ . The growth rate is constrained

$$b_{k,t,j} * v_{k,t,j} = g_{k,t,j} , \quad (4)$$

as the product of the current biomass abundance  $b_{k,t,j}$  and the growth rate constant  $v_{k,t,j}$ , which reflects 1<sup>st</sup>-order kinetics and can be tailored for the examined system. The stationary phenotype (not growing) mediates phenotypic transitions, which subtly delays phenotype transitions as a reflection of cellular delays (e.g. diffusion). Future biomass for the stationary phenotype is analogous to eq. (3),

$$b_{k,t,j} - \sum_s^S (es_s * (cvf_{k,t,j} - cvt_{k,t,j})) = b_{k,t+1,j} \quad (5)$$

except that a)  $g_{k,t,j} = 0$  by definition; b) the net transition to non-stationary phenotypes is negative; and c) all of the non-stationary strain phenotypes are summed for each species, since there are numerous non-stationary phenotypes yet only one stationary phenotype. The fraction of biomass that can transition is constrained

$$cvt_{k,t,j} \leq bcv * b_{k,t,j} + cvmin \quad (6)$$

to greater than a minimum limit ( $cxmin$ ) and lesser than a fraction of biomass ( $bcv$ ) above this minimum.

This constraint is an application of Heun's integration method [57, 58], which – for an arbitrary function  $y$ , its derivative  $y'$ , and a timestep  $\Delta t$  – is defined as

$$y_{t+1} = y_t + \frac{1}{2} * \Delta t * (y'_t + y'_{t+1}) . \quad (7)$$

This method is a 2<sup>nd</sup>-order Runge-Kutta formulation [59] that captures dynamic changes with high numerical accuracy [60] while maintaining a linear formulation that is amenable with our LP method.

Table 1: A glossary of dimensions, parameters, and variables that comprise the fitting model.

Term	Description
<b>DIMENSIONS</b>	
$s$	A species in the examined community. $j$ .
$k$	A growth phenotype of species $s$ .
$t$	An experimental time point.
$j$	An experimental trial.
$i$	Extracellular metabolite.
<b>PARAMETERS</b>	
$E_{s,t,j}$	The experimental growth signal for a species at instant $t$ in trial $j$ .
$es_{s,k}$	A boolean description of $k \in s$
$\Delta t$	The seconds per timestep, which determines the amount of biomass growth per timestep.
$n_{k,i}$	The exchange flux of each metabolite $i$ in each strain $k$ .
$v_{k,t,j}$	The rate constant for growth of strain $k$ at instant $t$ in trial $j$ . This parameter may be either a global value or a Michaelis-Menten flux such as $\frac{v_{max, k}}{k_m, k + c_{t,j,i}}$ that considers the concentration $c$ of $i$ .
$cvcf$ & $cvcf$	Conversion coefficients of phenotype biomass to and from the stationary phase, respectively.
$b_{cv_k}$	The greatest fraction of biomass ( $0 < bcv < 1$ ) of strain $k$ that can transition phenotypes in a timestep.
$cvmn$	The minimal value of variable $cvt_{k,t,j}$ .
<b>VARIABLES</b>	
$EC_k$	The conversion coefficient ( $0 < EC < 1000$ ) from parameter $E_{s,t,j}$ into biomass, which is unique for each strain $k$ .
$EB_{s,t,j}$	The computed biomass from each experimental datum, as the product of $EC_k$ & $E_{s,t,j}$ .
$b_{k,t,j}$	The predicted biomass from the fitting model.
$EV_{s,t,j}$	The variance between the computed experimental biomass $EB_{s,t,j}$ and the predicted biomass $b_{k,t,j}$ .
$c_{t,j,i}$	The concentration of metabolite $i$ at an experimental datum.
$g_{k,t,j}$	The predicted growth rate for each strain at each datum.
$cvt_{k,t,j}$ & $cvf_{k,t,j}$	The quantity of strain $k$ biomass that transitions to and from the stationary phase, respectively, at an experimental datum.

### 3.1.3 Concentrations

Future concentrations of substrates ( $c_{t+1,j,i}$ ) for all  $i \in I$  substrates are constrained

$$c_{t,j,i} + \frac{\Delta t}{2} \sum_k^K (n_{i,k}(g_{t,j,k} + g_{t+1,j,k})) = c_{t+1,j,i} \quad (8)$$

through Heun's integration method from eq. (7). This implementation includes the current concentration ( $c_{t,j,i}$ ) and concentration changes that are the product of  $\Delta t$  and the inner product of uptake fluxes ( $n_{i,k}$ ) – which are determined by simulating metabolic models [61] of each member – and the biomass growth rate for a member.

## 3.2 Objective

The objective function of the model

$$\sum_{s,t,j}^{S,T,J} (EV_{s,t,j}^2) - \sum_{k,t,j}^{k,t,j} (cvct * cvt_{k,t,j}) - \sum_{k,t,j}^{T,J,K} (cvcf * cvf_{k,t,j}) \quad (9)$$

minimizes both the sum of variance ( $EV$ ) from eq. (2) – between the predicted ( $b$ ) and experimentally calculated ( $EB$ ) biomass from eq. (10) – and the biomass transitions to  $cvct * cvt$  and from  $cvcf * cvf$  the stationary metabolic phase. This objective therefore optimally fits the data with the least phenotypic transitions, which prevents overfitting of the models with an unrealistic excess of phenotypic transitions, which presumes that metabolic transitions have a non-trivial cost to undertake.

## 3.3 Metabolic phenotypes

The phenotypes for each member, except for the stationary phase where no fluxes occur by definition, were designed from genome-scale metabolic models (GEM's) of the members. CommPhitting-compatible GEM's are constructed from experimental genomes through the ModelSEED pipeline [6]. The phenotypes for each species then leverage the corresponding species GEM through the following precise sequence of optimizations, constraints, and FBA simulations.

1. A minimal biomass growth and the environmental media are defined and constrained in the GEM, which includes prohibiting hydrogen consumption and limits oxygen consumption to twice the total consumption of the defining phenotype sources.
2. The total influx of carbonaceous compounds excluding the phenotype sources and compounds for which a formula is not defined was minimized. This optimally isolates the solution fluxes to only those that correspond with metabolism from the phenotype sources. The resultant fluxes from this minimization, excluding the phenotype sources, are fixed to the model and are unchanged in subsequent optimizations.
3. The total flux of the phenotype sources is minimized, which optimizes biomass yield from the phenotype sources. This presumably finds the most biologically desirable metabolic profile for this phenotype to which evolution has presumably steered the species' metabolome. The phenotype source fluxes from this minimization are fixed to the model.
4. Optionally, the excretion flux for assigned excreta of a phenotype (where experimental evidence is available) is maximized. The excreta flux from this maximization is fixed to the model.
5. The final step applies parsimonious FBA from COBRApy [61] – a method that minimizes the total flux and thereby finds the most efficient means of achieving defined metabolic goals – to the model while maintaining all of the aforementioned constraints and constants. This parsimonious simulation presumably emulates the efficiencies that evolution found for the simulated organism. The fluxes from this optimization are the phenotype fluxes that are employed by CommPhitting.

The above five-step optimization sequence is repeated for each phenotype of all species in the community. This robust method creates an irreducible metabolic profile for each phenotype that fosters pure phenotype predictions by CommPhitting.

### 3.4 E. coli-Psuedomonas competitive community

#### 3.4.1 Experimental Methods

The exemplary *P. fluorescens* SBW25 and *E. coli* (minimally modified) MG1655 community was selected for several reasons. Firstly, these members are model organisms that encompass a wide range of disciplines, such as a) the human microbiome, b) bioproduction, c) synthetic biology, d) the rhizosphere, e) agriculture, and f) ecology. Secondly, despite these members being robustly studied individually, have not been studied as a coculture, which both offers new experimental information and mitigates biases and preconceptions in hypothesis development and results interpretation.

The coculture was created through the following protocol. The *P. fluorescens* and *E. coli* strains were purchased from ATC, were stored at -80degC before preparation for electrocompetency, and were transformed with a plasmid to constitutively express either mNeongreen or mRuby2 fluorescent proteins (GFP and RFP), respectively [62]. Transformed cells were freshly streaked on a LB agar plate with appropriate antibiotics from -80degC glycerol stocks, and were incubated overnight at 30degC. A single colony from the plate was picked, placed into liquid LB (Lennox) broth with the antibiotics, and shaken @ 250 RPM overnight at 30degC. The 2 mL overnight culture was pelleted (4000x g for 10 min), the supernatant was removed, and the cells were resuspended in 1 mL of M9 media that contains no carbon source. This washing sequence was repeated twice. A 20  $\mu$ L aliquot of the washed cells was combined with 2 mL of M9 media that contained the appropriate carbon source for each strain – 10 mM D-maltose for *E. coli* and 6 mM 4-hydroxybenzoate for *P. fluorescens* – and was shaken @ 250 RPM for at least 16 hours. These overnight cultures were washed twice, following the same procedure as the overnight culture. These cells were finally analytically examined via optical density (OD 590 nm) and fluorescence using a plate reader (Hidex ...).

The aforementioned M9 cultured cells were mixed in fresh M9 media to achieve the desired initial cell ratio at OD 0.1 (590 nm) and carbon source concentration/ratios. A 200  $\mu$ L aliquot of the cell mixture was then added to wells of a sterile, black wall clear bottom, 96-well imaging plate (Costar). The 96-well plate was then added to a Hidex ... plate reader and was prewarmed to 30degC. The cells were shaken with (...) settings in the plate reader for, at least, 24h while being measured for optical density (600 nm), red fluorescence (544 excitation, 590 emission), and green fluorescence (485 excitation, 535 emission) every 10 minutes.

We utilized two methods to accurately disentangle the composition of a liquid coculture: 12 deg C and 37 deg C temperature variability and fluorescence reporter with the green- and red-fluorescence proteins, for *P. fluorescens* and *E. coli* respectively. The precision and mutual validation of these methods if depicted through the abar plates of Figure 2, which supports their application in our study as a resolving mechanism for the community members.

#### 3.4.2 Adapting the formulation for growth data

The general formulation in Section 3 was tailored to this particular 2-member community community in numerous aspects. First, the signal to biomass conversion constraint in eq. (10) was adapted to this community system

$$\begin{aligned} RFP_{t,j} * RFPC &= RFPB_{t,j} \\ GFP_{t,j} * GFPC &= GFPB_{t,j} \\ OD_{t,j} * ODC &= ODB_{t,j} \end{aligned} \quad (10)$$

where the *RFPC*, *GFPC*, and *ODC* conversion factors were defined for each member and for each  $RFP_{t,j}$ ,  $GFP_{t,j}$ , and  $OD_{t,j}$  experimental signal. Second, the variance constraint in eq. (2) is adapted for each experimental signal

$$\begin{aligned} RFPB_{t,j} - \sum_k^{K} (pf_k * b_{t,j,k}) &= RFPV_{t,j} \\ GFPB_{t,j} - \sum_k^{K} (ec_k * b_{t,j,k}) &= GFPV_{t,j} \\ OD_{t,j} - \sum_k^{K} (b_{t,j,k}) &= ODV_{t,j} \end{aligned} \quad (11)$$

where  $pf_k$  and  $ec_k$  are binary variables that filter biomass abundances for each member. Third, the objective function of eq. (9) is defined in terms of the experimental signals

$$\sum_{t,j}^{T,J} (EV_{ecoli,t,j}^2) + \sum_{t,j}^{T,J} (EV_{pseudo,t,j}^2) + \sum_{t,j}^{T,J} (EV_{OD,t,j}^2) - \sum_{k,t,j}^{T,J,K} (cvct * cvt_{k,t,j}) - \sum_{k,t,j}^{T,J,K} (cvcf * cvf_{k,t,j}) . \quad (12)$$

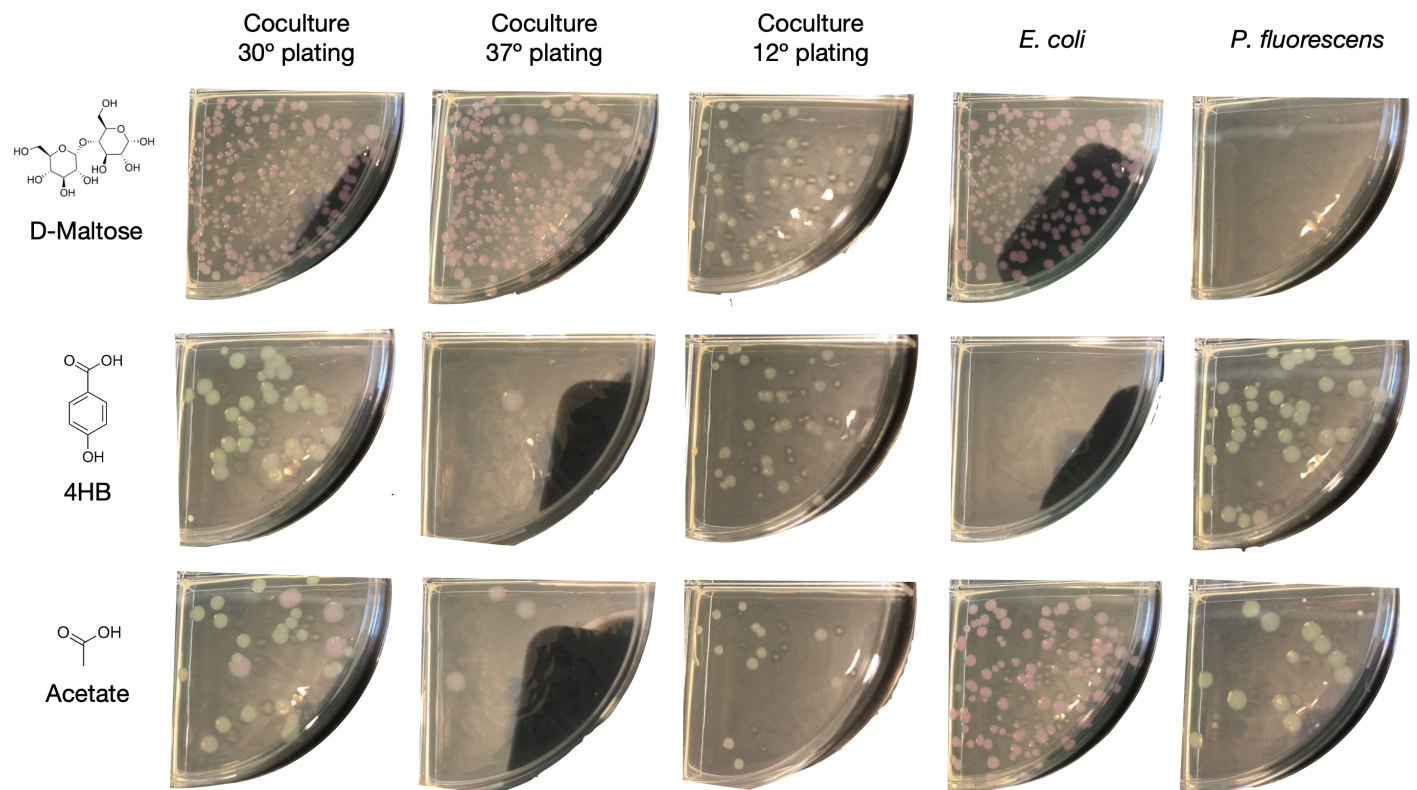


Figure 2: The agar growth from mono- and co-cultural experiments of *E. coli* and *P. fluorescens*. The similar growth profiles, and member exclusive conditions, between temperature and media compounds corroborates the application of fluorescence reporters to monitor member growth.

Finally, the data is filtered to remove content once the OD plateaus, at which point fluorescent proteins are over-produced by the stationary phase of the members. Specific timesteps and datums can also be removed to accommodate instances of bad trials or other experimental anomalies.

The *P. fluorescens* and *E. coli* genome-scale metabolic models were constructed in KBase Narrative 93465 through leveraging RAST to annotate the genomes [63] in the ModelSEED pipeline [64]. The *E. coli* model derived from the ASM584v2 experimental genome assembly and was gapfilled with acetate and maltose carbon sources that were studied. The *P. fluorescens* model derived from the ASM161270v1 experimental genome assembly and was gapfilled with acetate and 4-hydroxybenzoate carbon sources that were studied. This tailored formulation was further applied to BIOLOG experiments through defining the pertinent member phenotypes for each condition.

## 4 Results and Discussion

### 4.1 New data fitting method for iterative experimental design

The CommPhitting model was developed, through the aforementioned methods, to resolve phenotype abundances in microbial communities while maintaining flexibility to diverse experimental data types and structures. The logical workflow of the model is illustrated in Figure 3. Firstly, experimental data is parsed and parameterized into a dynamic optimization model of the community. Secondly, the model is simulated to the global optimum. Finally, the simulation predictions – namely phenotype abundances metabolic concentrations, and growth kinetic parameters – are expressed as figures or spreadsheets.

CommPhitting is composed as an open-source module in the Python language, principally leverages the Optlang optimization module [65] and the GLPK solver, and is amply documented as a component of the ModelSEEDpy library ModelSEEDpy ReadTheDocs. These attributes facilitate optimal accessibility for researchers and impact of our tool. CommPhitting is furthermore designed with robust graphing capabilities that succinctly communicate the high-dimensional simulation results in tables and figures, which accelerates basic understanding and applied engineering efforts by minimizing the data processing effort after each simulation to obtain meaningful insights.

### 4.2 Simulation insights

The CommPhitting simulations of our 2-member community fit the growth experimental data in Figure 4 remarkably well, and thus instills confidence in the model predictions. A slight anomaly in the experimental data of the maltose + 4HB trials in Figure 5 was accommodated by the method, and rendering these anomalous datums may have additional value for refining experimental procedures. The phenotype abundances in Figure ?? elucidated that [acetate] at just 100 nM triggers phenotypic changes in *Pseudomonas* that begin consuming the acetate instead of 4HB. This reinforces the postulated niche of *Pseudomonas*' as consuming overflow metabolism from conventional cCCR metabolic organisms such as *E. coli* [66] over consuming lignin degradation byproducts. This ecological role is further affirmed by BIOLOG experiments of the coculture, where growth is greater on organic acids – the prominent metabolite of overflow metabolism – than lignin derivatives such as 4HB.

The phenotype abundances further elucidate that the acetate and 4HB overall contribute approximately equally to the total *Pseudomonas* biomass despite that acetate is not provided in the media environmental of maltose and 4HB. These are actionable insights for rationally coupling community members based upon their measured, or here simulated, substrate preferences.

### 4.3 Validation

We validated the simulation predictions through a few approaches, which are illustrated in Figure \_\_\_. Firstly, the predicted concentration profiles in Figure 6 offered a relatively simple means of validating the simulation with metabolomics data. We accordingly measured [acetate] in the community and observed qualitative and quantitative alignment between the experimental and predicted concentrations, which are depicted in Figure \_\_\_. Secondly, the phenotype abundances were validated with transcriptomics data of the same experimental strains in similar environments to the metabolic phenotypes. Transcriptomics data was both sourced from literature [] for the \_\_\_ member(s) and were provided by in-house experiments where applicable literature was not found. These validation approaches via metabolomics and transcriptomics verify two separate domains of simulation predictions but their mutually consistency suggests that they may be redundant.

The minimal simulated growth of the acetate phenotype of *E. coli* in coculture with *P. fluorescens* motivated our examination of *E. coli* mutants that cannot absorb acetate to a) corroborate our experimental evidence that acetate is the

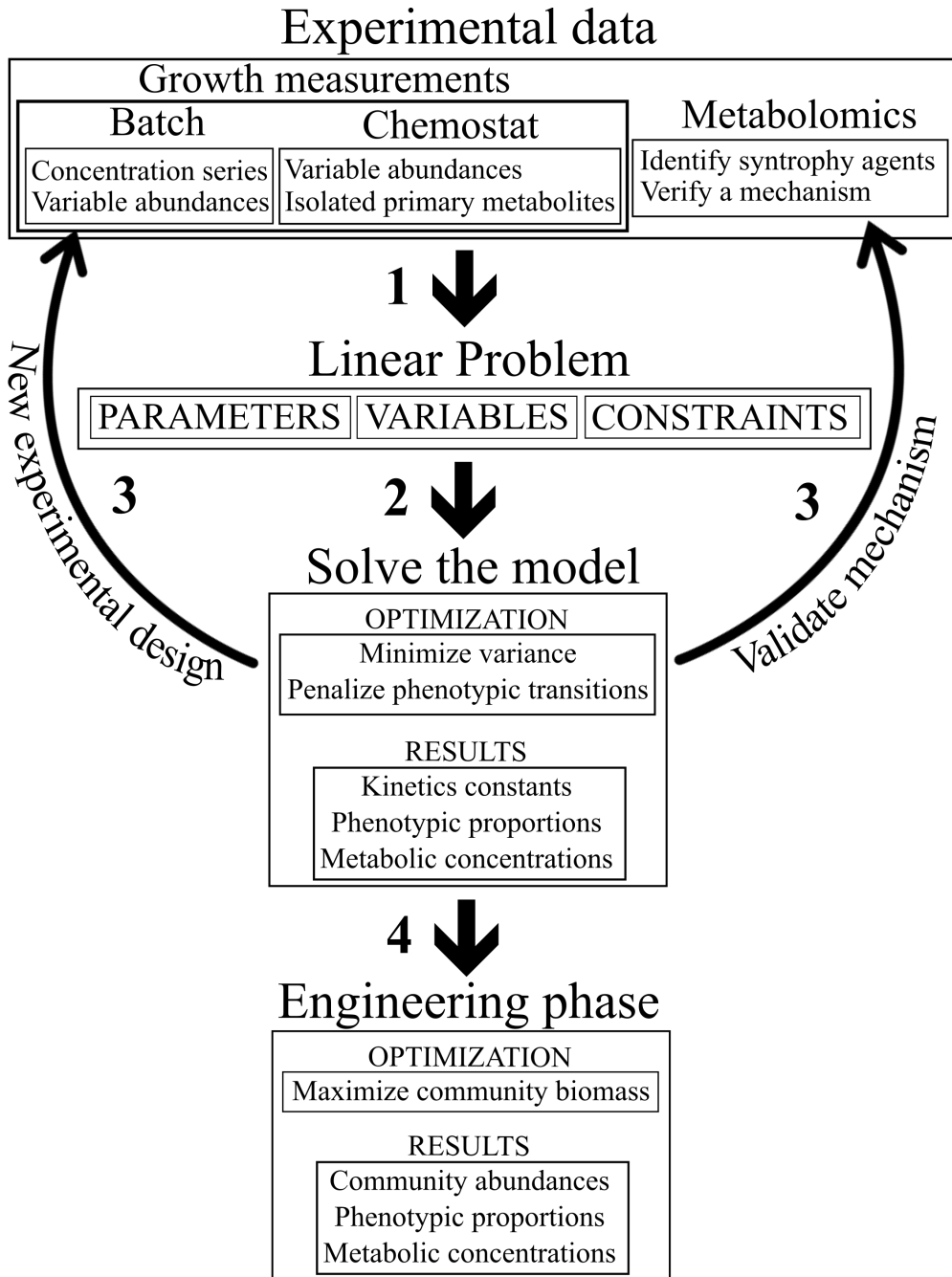


Figure 3: A workflow of the fitting model. **Step 1:** experimental data – from growth and possibly metabolomics measurements – is parsed into a linear problem that consists of the parameters and variables that are detailed in Table 1 and the constraints that are explained in Section 3. **Step 2:** the linear problem is executed with the objective function of eq. (9). **Step 3:** the simulation results are interpreted to either identify experimental changes that will improve modeling fit or to propose select metabolomic measurements that can crystallize mechanistic insights from the fit. Steps 1-3 repeat until a satisfactory fit and mechanistic resolution is achieved. **Step 4:** the fitted model can be used in a forward design-phase, instead of a purely retrospective fitting-phase, by replacing the objective function of the fitted model with one that optimizes for community growth. The system of steps 1-4 create an intricate method of gleaning mechanistic insights of microbial communities and then immediately using these insights to rationally design a community with desirable activity.

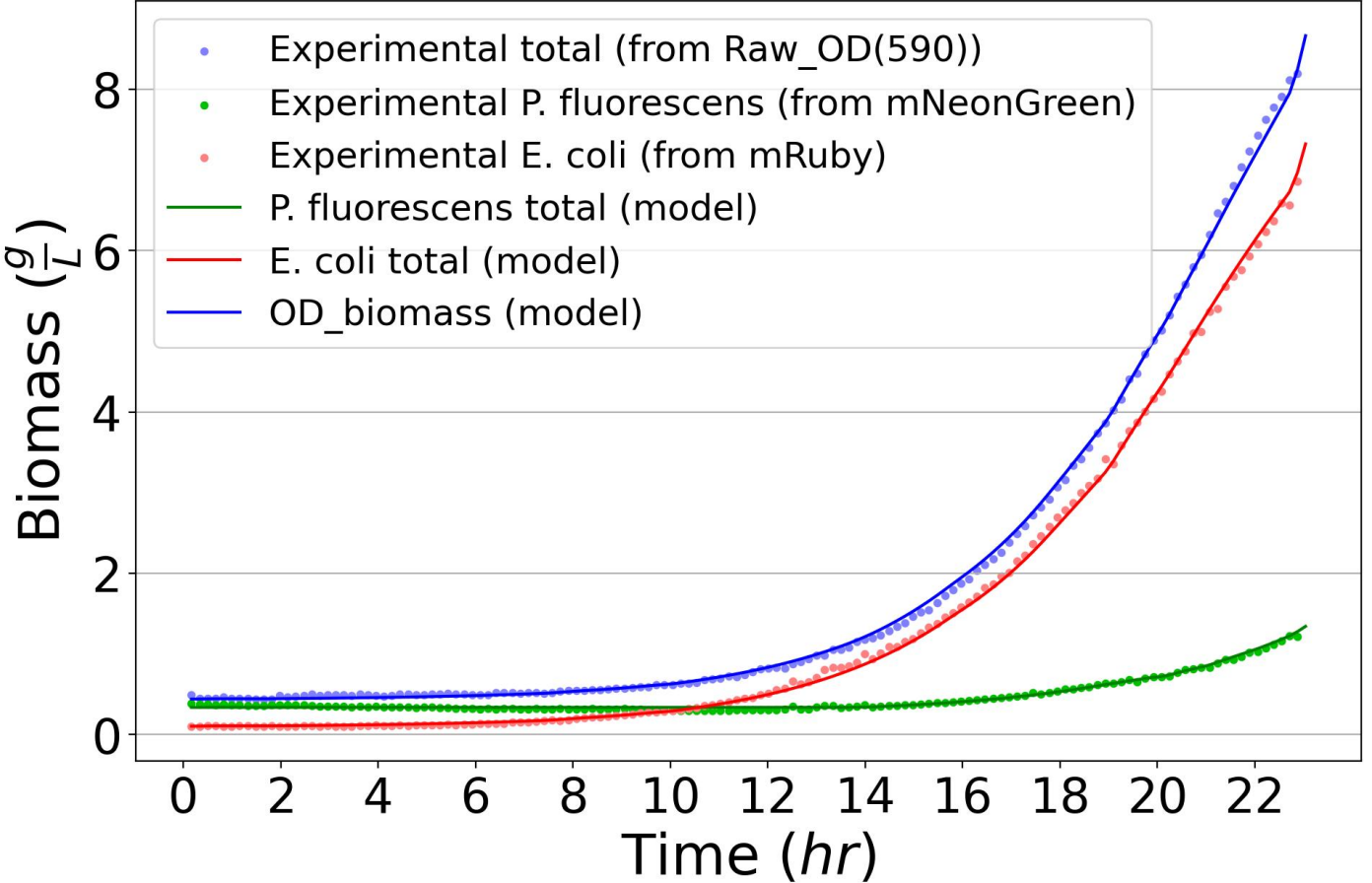


Figure 4: The converted experimental and predicted biomasses of the total community (OD), *E. coli* (RFP), and *P. fluorescens* (GFP) for the coculture experiment on maltose media (Table ??). Tight agreement between the experimental and predicted biomass values improves confidence in the predicted community behaviors and underlying chemical parameters.

Table 2: Table of final kinetic parameters predicted by model

predominate cross-feeding agent and b) that the prediction of minimal growth of the acetate phenotype. We purchased mutant knock-outs for the four proteins -- PoxB, ACS, Pta, and AckA – that contribute to acetate metabolism in MG1655 (see reference \_\_ figure \_\_) and examined their growth in an acetate coculture. A surprising discovery was that only the Pta knock-out actually terminated acetate consumption. The *E. coli* Pta knock-out, however, did not augment *P. fluorescens* growth relative to the wildtype *E. coli*, which supports that the wildtype *E. coli* was not appreciably consuming acetate and by extension the CommPhitting prediction of minimal acetate phenotype growth in the coculture.

## 5 Conclusion

Microbial communities influence myriad fields and offer untold potential for technology and industry; yet, our incomplete perception and understanding of member interactions hinders the precise engineering of microbial communities for these diverse applications. These interactions remain formiddable for experimental methods, where the combinatorial multitude of possible interactions is intractable, while existing computational methods have hereto improperly balanced mechanistic resolution for understanding the interactions or flexibility for accommodating available data sets. Our fitting method (CommPhitting) is proposed to balance resolution and flexibility to extract knowledge about community dynamics from only member genomes and -omics or growth data. The time-resolved predictions of metabolic concentrations in the

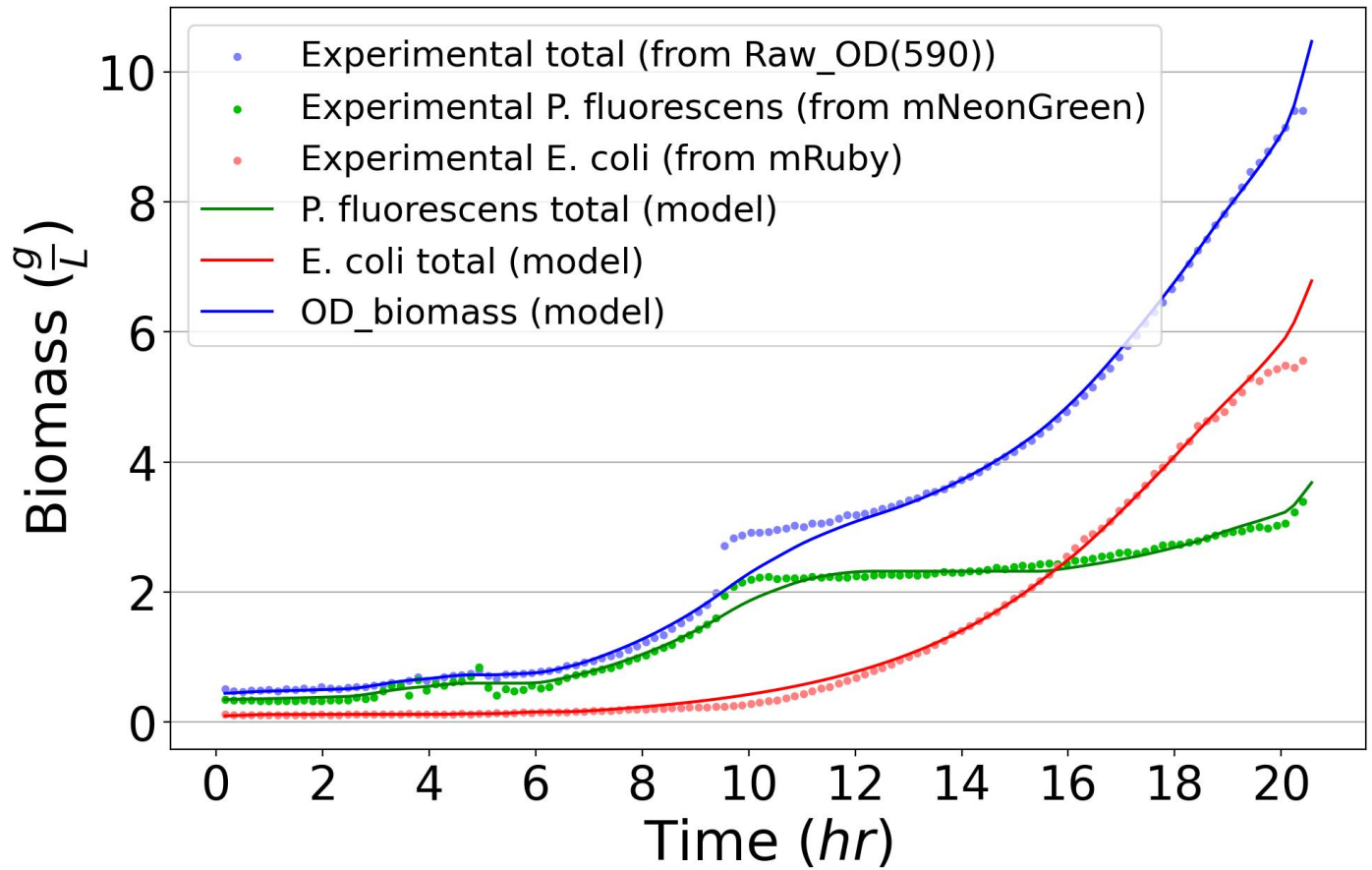


Figure 5: The converted experimental and predicted biomasses of the total community (OD), *E. coli* (RFP), and *P. fluorescens* (GFP) for the coculture experiment on maltose media (Table ??). Tight agreement between the experimental and predicted biomass values improves confidence in the predicted community behaviors and underlying chemical parameters.

images/G48\_cpd00179, cpd00029, cpd00136\_c.jpg

Figure 6: The concentrations of primary carbon sources maltose and 4HB, and the predominate cross-feeding agent acetate from the coculture trial of Figure 8. The dynamic production and subsequent consumption of acetate elicits the unique information that can be derived from CommPhitting simulations.

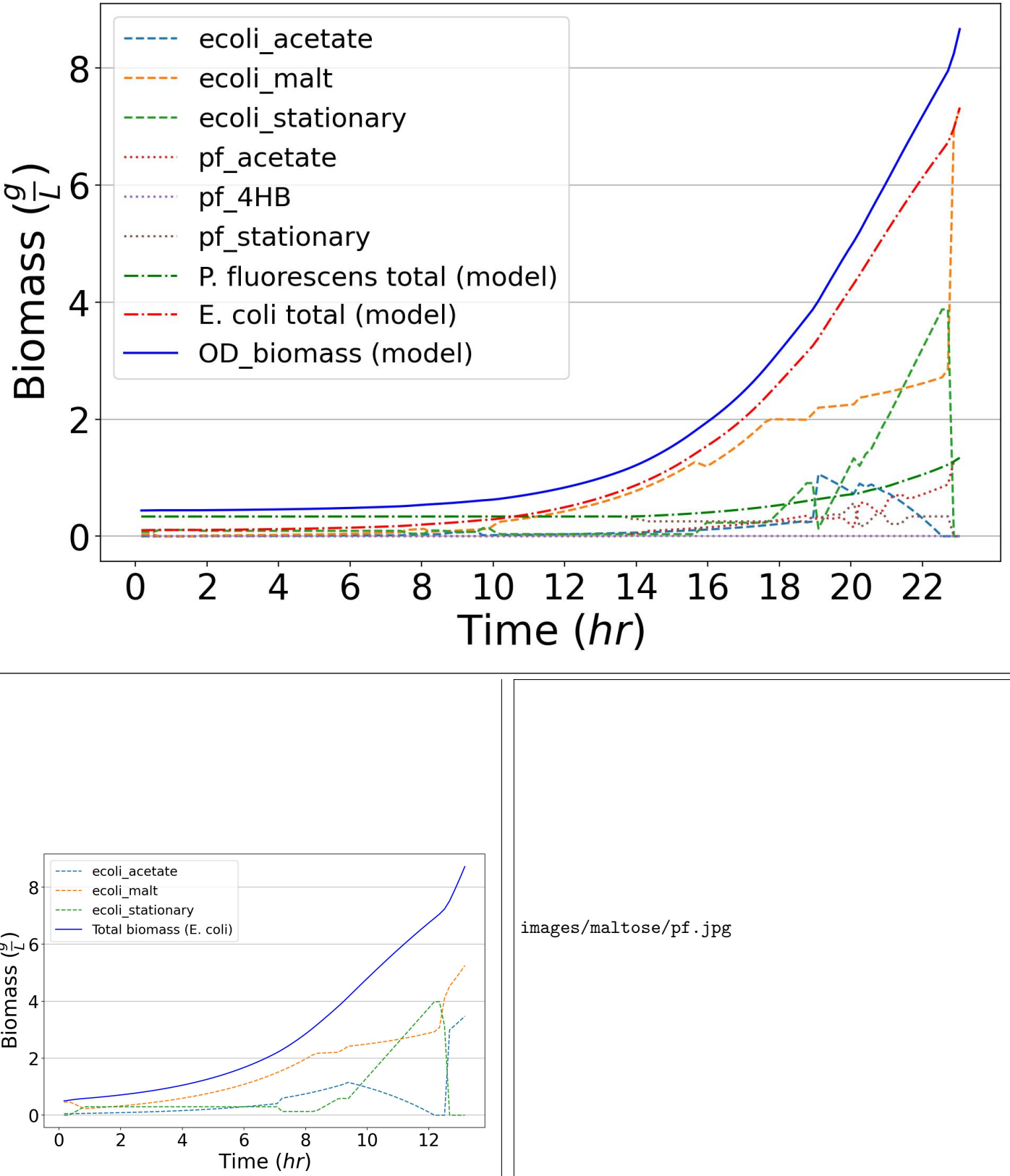


Figure 7: The phenotype abundances for an experiment with 5mM of maltose as the sole carbon sources. The top figure depicts the 1:1 coculture, where *E. coli* outcompeted *P. fluorescens*; however, *P. fluorescens* largely subsisted on the acetate excreta from *E. coli*. The bottom-right figure of *P. fluorescens* grown in isolation supports that *P. fluorescens* can grow on 4HB, albeit not as robustly as acetate. The bottom-left figure depicts *E. coli* grown in isolation, where it reaches the same final biomass but interestingly its acetate phenotype is much more active, as it tries to mitigate the inhibitory effects of acetate.

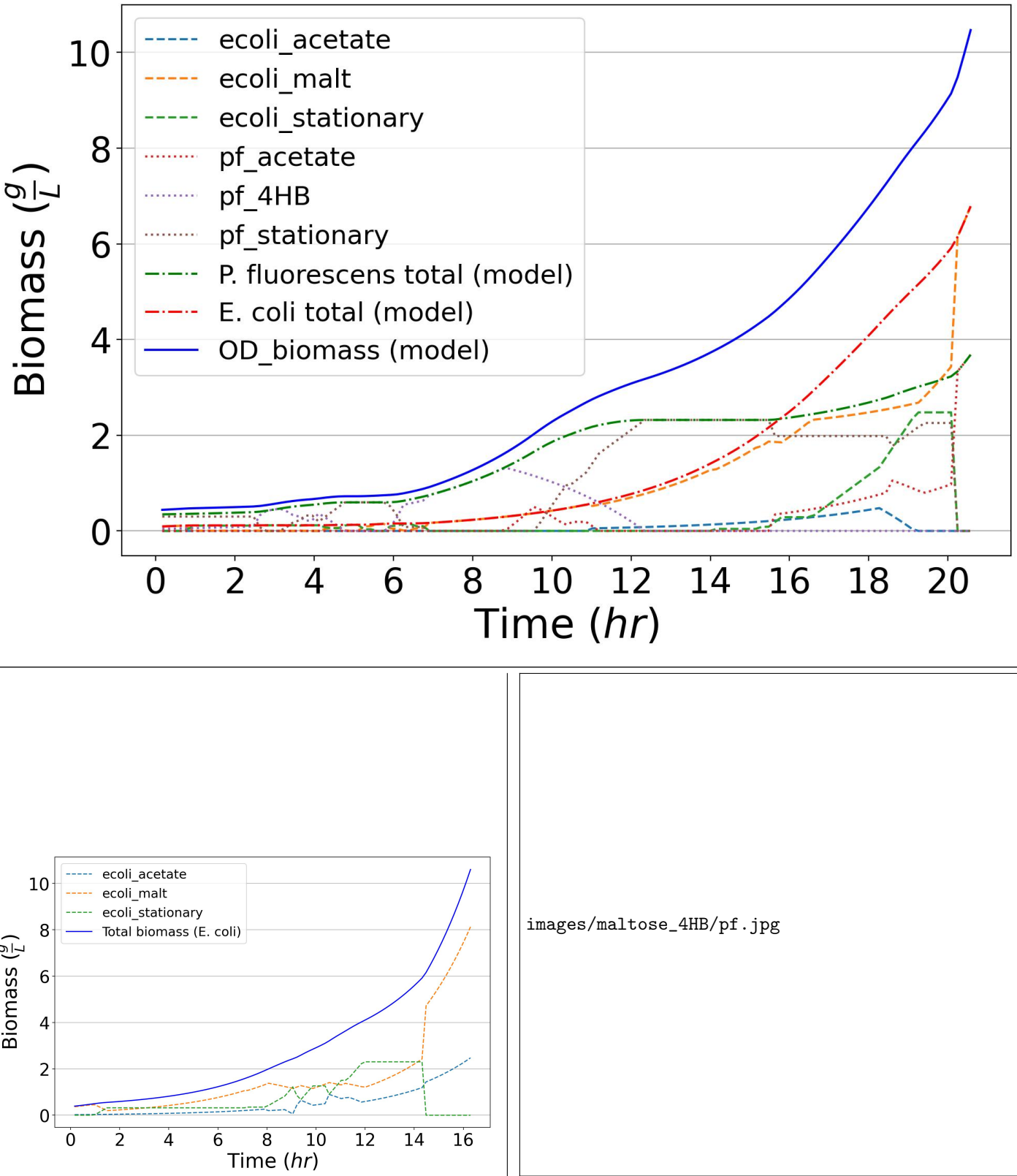


Figure 8: The phenotype abundances for an experiment with  $5mM$  of maltose and  $4mM$  of 4HB as the carbon sources. The top figure depicts the 1:1 coculture, where *E. coli* outcompeted *P. fluorescens*; however, *P. fluorescens* largely subsisted on the acetate excreta from *E. coli*. The bottom-right figure of *P. fluorescens* grown in isolation supports that *P. fluorescens* can grow on 4HB, albeit not as robustly as acetate. The bottom-left figure depicts *E. coli* grown in isolation, where it reaches the same final biomass but interestingly its acetate phenotype is much more active, as it tries to mitigate the inhibitory effects of acetate.

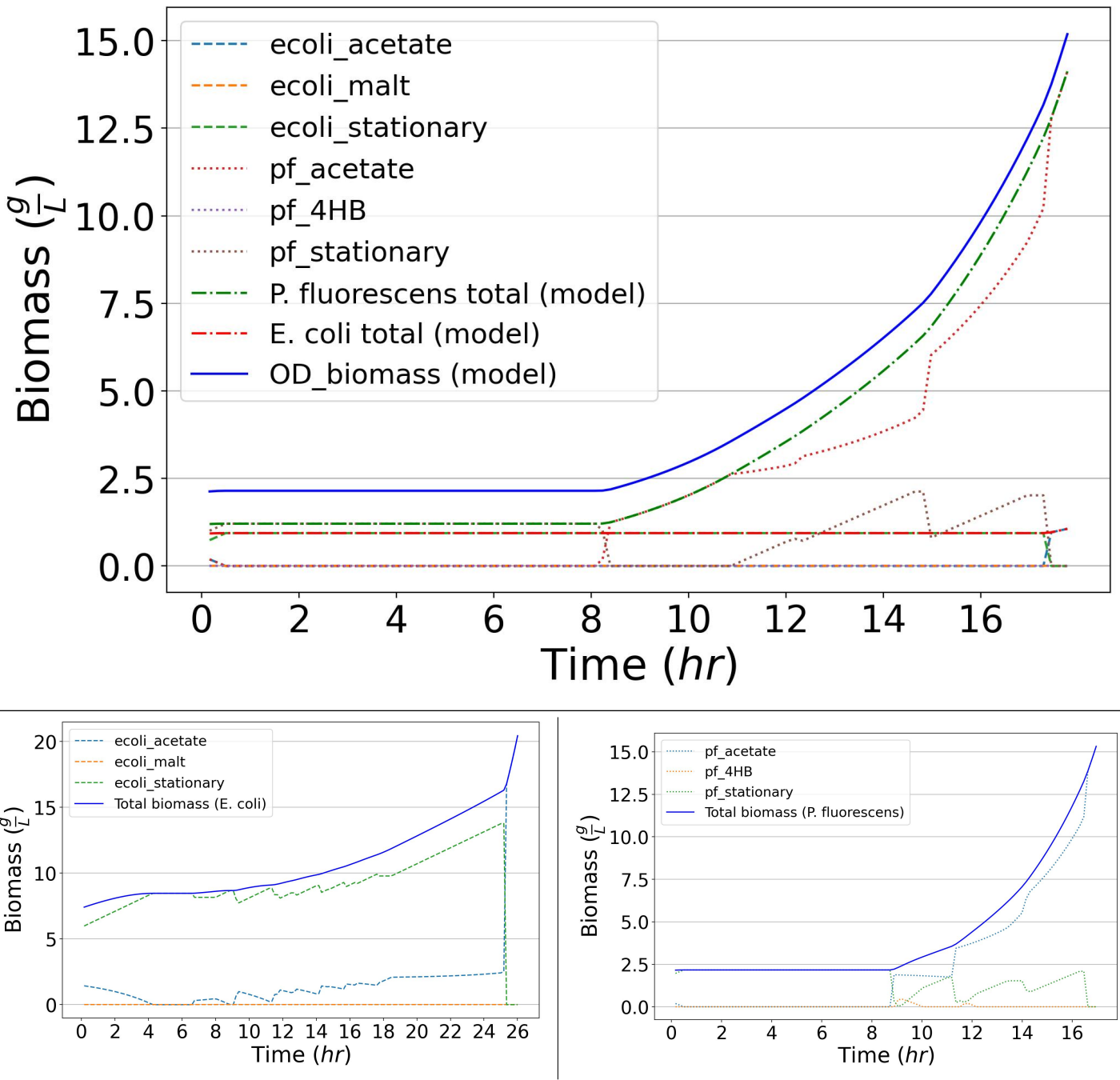


Figure 9: The phenotype abundances for an experiment with 50mM acetate as the sole carbon source. The top figure depicts the 1:1 coculture, where *E. coli* hardly grew while *P. fluorescens*. The bottom-right figure of *P. fluorescens* grown in isolation reveals that the total growth of *P. fluorescens* is unaffected by the presence of *E. coli* while it spends slightly more time in acetate growth phenotype in the presence of *E. coli*, perhaps as means of out-competing an adversary. The bottom-left figure depicts *E. coli* grown in isolation, where it is able to grow far more than in the presence of *P. fluorescens*, which supports the literature that *P. fluorescens* prefers, and it fiercely competitive with, consuming organic acids.

media, kinetic growth constants for each phenotype, and phenotype distributions within the community were validated with -omics data, which supports that the model adequately captures community biology.

The predictions from CommPhitting provide metabolic hypotheses, both qualitative and quantitative, with mechanistic support. This crucially allows researchers to judiciously direct limited resources to experiments and designs that exhibit the highest likelihood of success, thereby improving experimental efficiency and the rate of advancement towards synthesizing communities. Dissonance between predictions and experimental measurements can further be a source of actionable experimental hypotheses, such as disparate predicted and measurements concentrations that reflect a syntrophic interaction that is not embodied in the defined phenotype.

We envision that CommPhitting can be extended from the elucidation phase that we introduce herein, which cultivates basic understanding and hypothesis generation, to an exploration phase in Step 4 of Figure 3, where engineering hypotheses such as member mutations and environmental perturbations are simulated to predict community behaviors. The exploration phase would extend the elucidation phase by fixing the parameter and variable values that were derived from its fitting of experimental data and then exchange the optimization objective to suit the investigator's intention: e.g. phenotype or community abundance, bioproduction excreta, or total community growth. This prediction of behaviors in variable environments could further be applied to examine the effect of toxins/antibiotics. The exploration phase may then ultimately loop into the elucidation phase to complete a design/build/test/learn cycle [67] when an engineered community is experimentally measured and subsequently simulated via the elucidation phase to understand its new interactions. We therefore believe that CommPhitting can become an invaluable resource for expanding basic knowledge of community dynamics and ultimately engineering these communities for applications in fields as diverse as bioproduction, medical therapies, and national security.

## References

- [1] Stephen Nayfach, Simon Roux, Rekha Seshadri, Daniel Udwyar, Neha Varghese, Frederik Schulz, Dongying Wu, David Paez-Espino, I. Min Chen, Marcel Huntemann, Krishna Palaniappan, Joshua Ladau, Supratim Mukherjee, T. B.K. Reddy, Torben Nielsen, Edward Kirton, José P. Faria, Janaka N. Edirisinghe, Christopher S. Henry, Sean P. Jungbluth, Dylan Chivian, Paramvir Dehal, Elisha M. Wood-Charlson, Adam P. Arkin, Susannah G. Tringe, Axel Visel, Helena Abreu, Silvia G. Acinas, Eric Allen, Michelle A. Allen, Lauren V. Alteio, Gary Andersen, Alexandre M. Anesio, Graeme Attwood, Viridiana Avila-Magaña, Yacine Badis, Jake Bailey, Brett Baker, Petr Baldrian, Hazel A. Barton, David A.C. Beck, Eric D. Becraft, Harry R. Beller, J. Michael Beman, Rizlan Bernier-Latmani, Timothy D. Berry, Anthony Bertagnolli, Stefan Bertilsson, Jennifer M. Bhatnagar, Jordan T. Bird, Jeffrey L. Blanchard, Sara E. Blumer-Schutte, Brendan Bohannan, Mikayla A. Borton, Allyson Brady, Susan H. Brawley, Juliet Brodie, Steven Brown, Jennifer R. Brum, Andreas Brune, Donald A. Bryant, Alison Buchan, Daniel H. Buckley, Joy Buongiorno, Hinsby Cadillo-Quiroz, Sean M. Caffrey, Ashley N. Campbell, Barbara Campbell, Stephanie Carr, Jo Lynn Carroll, S. Craig Cary, Anna M. Cates, Rose Ann Cattolico, Ricardo Cavicchioli, Ludmila Chistoserdova, Maureen L. Coleman, Philippe Constant, Jonathan M. Conway, Walter P. Mac Cormack, Sean Crowe, Byron Crump, Cameron Currie, Rebecca Daly, Kristen M. DeAngelis, Vincent Denef, Stuart E. Denman, Adey Desta, Hebe Dionisi, Jeremy Dodsworth, Nina Dombrowski, Timothy Donohue, Mark Dopson, Timothy Driscoll, Peter Dunfield, Christopher L. Dupont, Katherine A. Dynarski, Virginia Edgcomb, Elizabeth A. Edwards, Mostafa S. Elshahed, Israel Figueroa, Beverly Flood, Nathaniel Fortney, Caroline S. Fortunato, Christopher Francis, Claire M.M. Gachon, Sarahi L. Garcia, Maria C. Gazitua, Terry Gentry, Lena Gerwick, Javad Gharechahi, Peter Girguis, John Gladden, Mary Gradovalle, Stephen E. Grasby, Kelly Gravuer, Christen L. Grettenberger, Robert J. Gruninger, Jiarong Guo, Mussie Y. Habteselassie, Steven J. Hallam, Roland Hatzenpichler, Bela Hausmann, Terry C. Hazen, Brian Hedlund, Cynthia Henny, Lydie Herfort, Maria Hernandez, Olivia S. Hershey, Matthias Hess, Emily B. Hollister, Laura A. Hug, Dana Hunt, Janet Jansson, Jessica Jarett, Vitaly V. Kadnikov, Charlene Kelly, Robert Kelly, William Kelly, Cheryl A. Kerfeld, Jeff Kimbrel, Jonathan L. Klassen, Konstantinos T. Konstantinidis, Laura L. Lee, Wen Jun Li, Andrew J. Loder, Alexander Loy, Mariana Lozada, Barbara MacGregor, Cara Magnabosco, Aline Maria da Silva, R. Michael McKay, Katherine McMahon, Chris S. McSweeney, Mónica Medina, Laura Meredith, Jessica Mizzi, Thomas Mock, Lily Momper, Mary Ann Moran, Connor Morgan-Lang, Duane Moser, Gerard Muyzer, David Myrold, Maisie Nash, Camilla L. Nesbø, Anthony P. Neumann, Rebecca B. Neumann, Daniel Noguera, Trent Northen, Jeanette Norton, Brent Nowinski, Klaus Nüsslein, Michelle A. O'Malley, Rafael S. Oliveira, Valeria Maia de Oliveira, Tullis Onstott, Jay Osvatic, Yang Ouyang, Maria Pachiadaki, Jacob Parnell, Laila P. Partida-Martinez, Kabir G. Peay, Dale Pelletier, Xuefeng Peng, Michael Pester, Jennifer Pett-Ridge, Sari Peura, Petra Pjevac, Alvaro M. Plominsky, Anja Poehlein, Phillip B. Pope, Nikolai Ravin, Molly C. Redmond, Rebecca Reiss, Virginia Rich, Christian Rinke, Jorge L. Mazza Rodrigues, William Rodriguez-Reillo, Karen Rossmassler, Joshua Sackett, Ghasem Hosseini Salekdeh, Scott Saleska, Matthew Scarborough, Daniel Schachtman, Christopher W. Schadt, Matthew Schrenk, Alexander Sczyrba, Aditi

- Sengupta, Joao C. Setubal, Ashley Shade, Christine Sharp, David H. Sherman, Olga V. Shubenkova, Isabel Natalia Sierra-Garcia, Rachel Simister, Holly Simon, Sara Sjöling, Joan Slonczewski, Rafael Soares Correa de Souza, John R. Spear, James C. Stegen, Ramunas Stepanauskas, Frank Stewart, Garret Suen, Matthew Sullivan, Dawn Sumner, Brandon K. Swan, Wesley Swingley, Jonathan Tarn, Gordon T. Taylor, Hanno Teeling, Memory Tekere, Andreas Teske, Torsten Thomas, Cameron Thrash, James Tiedje, Claire S. Ting, Benjamin Tully, Gene Tyson, Osvaldo Ulloa, David L. Valentine, Marc W. Van Goethem, Jean VanderGheynst, Tobin J. Verbeke, John Vollmers, Aurèle Vuillemin, Nicholas B. Waldo, David A. Walsh, Bart C. Weimer, Thea Whitman, Paul van der Wielen, Michael Wilkins, Timothy J. Williams, Ben Woodcroft, Jamie Wootton, Kelly Wrighton, Jun Ye, Erica B. Young, Noha H. Youssef, Feiqiao Brian Yu, Tamara I. Zemskaya, Ryan Ziels, Tanja Woyke, Nigel J. Mouncey, Natalia N. Ivanova, Nikos C. Kyripides, and Emiley A. Eloe-Fadrosh. A genomic catalog of Earth's microbiomes. *Nature Biotechnology*, 39(4):499–509, 2021. ISSN 15461696. doi: 10.1038/s41587-020-0718-6.
- [2] Saeed Shoae, Pouyan Ghaffari, Petia Kovatcheva-Datchary, Adil Mardinoglu, Partho Sen, Estelle Pujos-Guillot, Tomas De Wouters, Catherine Juste, Salwa Rizkalla, Julien Chilloux, Lesley Hoyles, Jeremy K. Nicholson, Joel Dore, Marc E. Dumas, Karine Clement, Fredrik Bäckhed, and Jens Nielsen. Quantifying Diet-Induced Metabolic Changes of the Human Gut Microbiome. *Cell Metabolism*, 22(2):320–331, 2015. ISSN 19327420. doi: 10.1016/j.cmet.2015.07.001.
  - [3] Manish Kumar, Boyang Ji, Karsten Zengler, and Jens Nielsen. Modelling approaches for studying the microbiome. *Nature Microbiology*, 4(8):1253–1267, 2019. ISSN 20585276. doi: 10.1038/s41564-019-0491-9. URL <http://dx.doi.org/10.1038/s41564-019-0491-9>.
  - [4] Saeed Shoae, Fredrik Karlsson, Adil Mardinoglu, Intawat Nookaew, Sergio Bordel, and Jens Nielsen. Understanding the interactions between bacteria in the human gut through metabolic modeling. *Scientific Reports*, 3:1–10, 2013. ISSN 20452322. doi: 10.1038/srep02532.
  - [5] Luke Mcguigan and Máire Callaghan. The evolving dynamics of the microbial community in the cystic fibrosis lung. *Environmental Microbiology*, 17(1):16–28, 2015. ISSN 14622920. doi: 10.1111/1462-2920.12504.
  - [6] Howard F. Jenkinson and Richard J. Lamont. Oral microbial communities in sickness and in health. *Trends in Microbiology*, 13(12):589–595, 2005. ISSN 0966842X. doi: 10.1016/j.tim.2005.09.006.
  - [7] Robin K. Pettit. Mixed fermentation for natural product drug discovery. *Applied Microbiology and Biotechnology*, 83(1):19–25, 2009. ISSN 01757598. doi: 10.1007/s00253-009-1916-9.
  - [8] Ethan T. Hillman, Louis Edwards Caceres-Martinez, Gozdem Kilaz, and Kevin V. Solomon. Top-down enrichment of oil field microbiomes to limit souring and control oil composition during extraction operations. *AIChE Journal*, (September):1–13, 2022. ISSN 15475905. doi: 10.1002/aic.17927.
  - [9] Bryan S. Griffiths and Laurent Philippot. Insights into the resistance and resilience of the soil microbial community. *FEMS Microbiology Reviews*, 37(2):112–129, 2013. ISSN 01686445. doi: 10.1111/j.1574-6976.2012.00343.x.
  - [10] William B. Whitman, David C. Coleman, and William J. Wiebe. Prokaryotes: The unseen majority. *Proceedings of the National Academy of Sciences of the United States of America*, 95(12):6578–6583, 1998. ISSN 00278424. doi: 10.1073/pnas.95.12.6578.
  - [11] Anne E. Dukas, Rachel S. Poretsky, and Victoria J. Orphan. Deep-Sea Archaea Fix and Share Nitrogen in Methane-Consuming Microbial Consortia. *Science*, 326(October):422–427, 2009.
  - [12] Xuesong He, Jeffrey S. McLean, Lihong Guo, Renate Lux, and Wenyuan Shi. The social structure of microbial community involved in colonization resistance. *ISME Journal*, 8(3):564–574, 2014. ISSN 17517370. doi: 10.1038/ismej.2013.172.
  - [13] Daniel van der Lelie, Akihiko Oka, Safiyh Taghavi, Junji Umeno, Ting Jia Fan, Katherine E. Merrell, Sarah D. Watson, Lisa Ouellette, Bo Liu, Muyiwa Awoniyi, Yunjia Lai, Liang Chi, Kun Lu, Christopher S. Henry, and R. Balfour Sartor. Rationally designed bacterial consortia to treat chronic immune-mediated colitis and restore intestinal homeostasis. *Nature Communications*, 12(1):1–17, 2021. ISSN 20411723. doi: 10.1038/s41467-021-23460-x.
  - [14] Ricardo Cavichioli, William J. Ripple, Kenneth N. Timmis, Farooq Azam, Lars R. Bakken, Matthew Baylis, Michael J. Behrenfeld, Antje Boetius, Philip W. Boyd, Aimée T. Classen, Thomas W. Crowther, Roberto Danovaro, Christine M. Foreman, Jef Huisman, David A. Hutchins, Janet K. Jansson, David M. Karl, Britt Koskella, David B.

- Mark Welch, Jennifer B.H. Martiny, Mary Ann Moran, Victoria J. Orphan, David S. Reay, Justin V. Remais, Virginia I. Rich, Brajesh K. Singh, Lisa Y. Stein, Frank J. Stewart, Matthew B. Sullivan, Madeleine J.H. van Oppen, Scott C. Weaver, Eric A. Webb, and Nicole S. Webster. Scientists' warning to humanity: microorganisms and climate change. *Nature Reviews Microbiology*, 17(9):569–586, 2019. ISSN 17401534. doi: 10.1038/s41579-019-0222-5. URL <http://dx.doi.org/10.1038/s41579-019-0222-5>.
- [15] V. J. Orphan, C. H. House, K. U. Hinrichs, K. D. McKeegan, and E. F. DeLong. Methane-consuming archaea revealed by directly coupled isotopic and phylogenetic analysis. *Science*, 293(5529):484–487, 2001. ISSN 00368075. doi: 10.1126/science.1061338.
- [16] Jennifer B. Glass and Victoria J. Orphan. Trace metal requirements for microbial enzymes involved in the production and consumption of methane and nitrous oxide. *Frontiers in Microbiology*, 3(FEB):1–20, 2012. ISSN 1664302X. doi: 10.3389/fmicb.2012.00061.
- [17] Jacob D. Palmer and Kevin R. Foster. Bacterial species rarely work together. *Science*, 376(6593):581–582, 2022. ISSN 10959203. doi: 10.1126/science.abn5093.
- [18] Cristiane Aparecida Pereira, Rogério Lima Romeiro, Anna Carolina Borges Pereira Costa, Ana Karina Silva MacHado, Juliana Campos Junqueira, and Antonio Olavo Cardoso Jorge. Susceptibility of *Candida albicans*, *Staphylococcus aureus*, and *Streptococcus mutans* biofilms to photodynamic inactivation: An in vitro study. *Lasers in Medical Science*, 26(3):341–348, 2011. ISSN 02688921. doi: 10.1007/s10103-010-0852-3.
- [19] Thien Fah C. Mah and George A. O'Toole. Mechanisms of biofilm resistance to antimicrobial agents. *Trends in Microbiology*, 9(1):34–39, 2001. ISSN 0966842X. doi: 10.1016/S0966-842X(00)01913-2.
- [20] K. Sauer, M. C. Cullen, A. H. Rickard, L. A.H. Zeef, D. G. Davies, and P. Gilbert. Characterization of nutrient-induced dispersion in *Pseudomonas aeruginosa* PAO1 biofilm. *Journal of Bacteriology*, 186(21):7312–7326, 2004. ISSN 00219193. doi: 10.1128/JB.186.21.7312-7326.2004.
- [21] Prashanth Suntharalingam and Dennis G. Cvitkovitch. Quorum sensing in streptococcal biofilm formation. *Trends in Microbiology*, 13(1):3–6, 2005. ISSN 0966842X. doi: 10.1016/j.tim.2004.11.009.
- [22] Michael T. Mee, James J. Collins, George M. Church, and Harris H. Wang. Syntrophic exchange in synthetic microbial communities. *Proceedings of the National Academy of Sciences of the United States of America*, 111(20), 2014. ISSN 10916490. doi: 10.1073/pnas.1405641111.
- [23] Samay Pande, Holger Merker, Katrin Bohl, Michael Reichelt, Stefan Schuster, Luís F. De Figueiredo, Christoph Kaleta, and Christian Kost. Fitness and stability of obligate cross-feeding interactions that emerge upon gene loss in bacteria. *ISME Journal*, 8(5):953–962, 2014. ISSN 17517370. doi: 10.1038/ismej.2013.211.
- [24] Erica C. Seth and Michiko E. Taga. Nutrient cross-feeding in the microbial world. *Frontiers in Microbiology*, 5 (JULY):1–6, 2014. ISSN 1664302X. doi: 10.3389/fmicb.2014.00350.
- [25] Edwin H. Wintermute and Pamela A. Silver. Emergent cooperation in microbial metabolism. *Molecular Systems Biology*, 6(407):1–7, 2010. ISSN 17444292. doi: 10.1038/msb.2010.66. URL <http://dx.doi.org/10.1038/msb.2010.66>.
- [26] Jack A. Connolly, William R. Harcombe, Michael J. Smanski, Linda L. Kinkel, Eriko Takano, and Rainer Breitling. Harnessing intercellular signals to engineer the soil microbiome. *Natural Product Reports*, 39(2):311–324, 2022. ISSN 14604752. doi: 10.1039/d1np00034a.
- [27] Cristal Zuñiga, Tingting Li, Michael T. Guarnieri, Jackson P. Jenkins, Chien Ting Li, Kerem Bingol, Young Mo Kim, Michael J. Betenbaugh, and Karsten Zengler. Synthetic microbial communities of heterotrophs and phototrophs facilitate sustainable growth. *Nature Communications*, 11(1), 2020. ISSN 20411723. doi: 10.1038/s41467-020-17612-8. URL <http://dx.doi.org/10.1038/s41467-020-17612-8>.
- [28] Nikodimos A. Gebreselassie and Maciek R. Antoniewicz.  $^{13}\text{C}$ -metabolic flux analysis of co-cultures: A novel approach. *Metabolic Engineering*, 31:132–139, 2015. ISSN 10967184. doi: 10.1016/j.ymben.2015.07.005. URL <http://dx.doi.org/10.1016/j.ymben.2015.07.005>.
- [29] R Frank Rosenzweig, R R Sharp, David S Treves, and Julian Adams. Microbial evolution in a simple unstructured environment: Genetic differentiation in *Escherichia coli*. *Genetics Society of America*, 137:903–917, 1994.

- [30] Jeffrey D. Orth, Ines Thiele, and Bernhard O. Palsson. What is flux balance analysis? *Nature Biotechnology*, 28(3): 245–248, 2010. ISSN 10870156. doi: 10.1038/nbt.1614.
- [31] Eugen Bauer, Johannes Zimmermann, Federico Baldini, Ines Thiele, and Christoph Kaleta. BacArena: Individual-based metabolic modeling of heterogeneous microbes in complex communities. *PLoS Computational Biology*, 13(5): 1–22, 2017. ISSN 15537358. doi: 10.1371/journal.pcbi.1005544.
- [32] Denny Popp and Florian Centler.  $\mu$ BialSim: Constraint-Based Dynamic Simulation of Complex Microbiomes. *Frontiers in Bioengineering and Biotechnology*, 8(June), 2020. ISSN 22964185. doi: 10.3389/fbioe.2020.00574.
- [33] Ali R. Zomorodi, Mohammad Mazharul Islam, and Costas D. Maranas. D-OptCom: Dynamic Multi-level and Multi-objective Metabolic Modeling of Microbial Communities. *ACS Synthetic Biology*, 3(4):247–257, 2014. ISSN 21615063. doi: 10.1021/sb4001307.
- [34] Aleksej Zelezniak, Sergej Andrejev, Olga Ponomarova, Daniel R. Mende, Peer Bork, and Kiran Raosaheb Patil. Metabolic dependencies drive species co-occurrence in diverse microbial communities. *Proceedings of the National Academy of Sciences of the United States of America*, 112(20):6449–6454, 2015. ISSN 10916490. doi: 10.1073/pnas.1421834112.
- [35] Christian Diener, Sean M. Gibbons, and Osbaldo Resendis-Antonio. MICOM: Metagenome-Scale Modeling To Infer Metabolic Interactions in the Gut Microbiota. *mSystems*, 5(1), 2020. ISSN 2379-5077. doi: 10.1128/msystems.00606-19.
- [36] Daniel R. Hyduke, Nathan E. Lewis, and Bernhard O. Palsson. Analysis of omics data with genome-scale models of metabolism. *Molecular BioSystems*, 9(2):167–174, 2013. ISSN 1742206X. doi: 10.1039/c2mb25453k.
- [37] Robert A. Dromms and Mark P. Styczynski. Systematic applications of metabolomics in metabolic engineering. *Metabolites*, 2(4):1090–1122, 2012. ISSN 22181989. doi: 10.3390/metabo2041090.
- [38] Xuewen Chen, Ana P. Alonso, Doug K. Allen, Jennifer L. Reed, and Yair Shachar-Hill. Synergy between  $^{13}\text{C}$ -metabolic flux analysis and flux balance analysis for understanding metabolic adaption to anaerobiosis in *E. coli*. *Metabolic Engineering*, 13(1):38–48, 2011. ISSN 10967176. doi: 10.1016/j.ymben.2010.11.004. URL <http://dx.doi.org/10.1016/j.ymben.2010.11.004>.
- [39] Keren Yizhak, Tomer Benyaminini, Wolfram Liebermeister, Eytan Ruppin, and Tomer Shlomi. Integrating quantitative proteomics and metabolomics with a genome-scale metabolic network model. *Bioinformatics*, 26(12):255–260, 2010. ISSN 13674803. doi: 10.1093/bioinformatics/btq183.
- [40] Weihua Guo and Xueyang Feng. OM-FBA: Integrate transcriptomics data with flux balance analysis to decipher the cell metabolism. *PLoS ONE*, 11(4):1–20, 2016. ISSN 19326203. doi: 10.1371/journal.pone.0154188.
- [41] Rogier J.P. Van Berlo, Dick De Ridder, Jean Marc Daran, Pascale A.S. Daran-Lapujade, Bas Teusink, and Marcel J.T. Reinders. Predicting metabolic fluxes using gene expression differences as constraints. *IEEE/ACM Transactions on Computational Biology and Bioinformatics*, 8(1):206–216, 2011. ISSN 15455963. doi: 10.1109/TCBB.2009.55.
- [42] Min Kyung Kim and Desmond S. Lun. Methods for integration of transcriptomic data in genome-scale metabolic models. *Computational and Structural Biotechnology Journal*, 11(18):59–65, 2014. ISSN 20010370. doi: 10.1016/j.csbj.2014.08.009. URL <http://dx.doi.org/10.1016/j.csbj.2014.08.009>.
- [43] Vikash Pandey, Daniel Hernandez Gardiol, Anush Chiappino-pepe, and Vassily Hatzimanikatis. TEX-FBA : A constraint-based method for integrating gene expression , thermodynamics , and metabolomics data into genome-scale metabolic models. *bioRxiv*, pages 1–30, 2019.
- [44] Davide Chicco. Ten quick tips for machine learning in computational biology. *BioData Mining*, 10(1):1–17, 2017. ISSN 17560381. doi: 10.1186/s13040-017-0155-3.
- [45] David T. Jones. Setting the standards for machine learning in biology. *Nature Reviews Molecular Cell Biology*, 20(11):659–660, 2019. ISSN 14710080. doi: 10.1038/s41580-019-0176-5. URL <http://dx.doi.org/10.1038/s41580-019-0176-5>.
- [46] Eva Maria Kapfer, Paul Stapor, and Jan Hasenauer. Challenges in the calibration of large-scale ordinary differential equation models. *IFAC-PapersOnLine*, 52(26):58–64, 2019. ISSN 24058963. doi: 10.1016/j.ifacol.2019.12.236. URL <https://doi.org/10.1016/j.ifacol.2019.12.236>.

- [47] Laura Lee, David Atkinson, Andrew G. Hirst, and Stephen J. Cornell. A new framework for growth curve fitting based on the von Bertalanffy Growth Function. *Scientific Reports*, 10(1):1–12, 2020. ISSN 20452322. doi: 10.1038/s41598-020-64839-y.
- [48] Jon E. Lindstrom, Ronald P. Barry, and Joan F. Braddock. Microbial community analysis: A kinetic approach to constructing potential C source utilization patterns. *Soil Biology and Biochemistry*, 30(2):231–239, 1997. ISSN 00380717. doi: 10.1016/S0038-0717(97)00113-2.
- [49] J L Garland. Potential and limitations of BIOLOG for microbial community analysis. *Microbial Biosystems: New Frontiers, Proceedings of the 8th International Symposium on Microbial Ecology*, pages 1–7, 1999. ISSN 1642395X.
- [50] Saratram Gopalakrishnan, Satyakam Dash, and Costas Maranas. K-FIT: An accelerated kinetic parameterization algorithm using steady-state fluxomic data. *Metabolic Engineering*, 61(January):197–205, 2020. ISSN 10967184. doi: 10.1016/j.ymben.2020.03.001.
- [51] Jared L Gearhart, Kristin L Adair, Richard J Detry, Justin D Durfee, Katherine A Jones, and Nathaniel Martin. Comparison of Open-Source Linear Programming Solvers. Report SAND2013-8847. (October):62, 2013. URL <http://www.ntis.gov/help/ordermethods.asp?loc=7-4-0#online>.
- [52] A. Cassioli, D. Di Lorenzo, M. Locatelli, F. Schoen, and M. Sciandrone. Machine learning for global optimization. *Computational Optimization and Applications*, 51(1):279–303, 2012. ISSN 09266003. doi: 10.1007/s10589-010-9330-x.
- [53] Fernando Rojo. Carbon catabolite repression in *Pseudomonas*: Optimizing metabolic versatility and interactions with the environment. *FEMS Microbiology Reviews*, 34(5):658–684, 2010. ISSN 01686445. doi: 10.1111/j.1574-6976.2010.00218.x.
- [54] Hans C. Bernstein. Reconciling Ecological and Engineering Design Principles for Building Microbiomes. *mSystems*, 4(3):1–5, 2019. ISSN 23795077. doi: 10.1128/msystems.00106-19.
- [55] Tanya Barrett, Dennis B. Troup, Stephen E. Wilhite, Pierre Ledoux, Dmitry Rudnev, Carlos Evangelista, Irene F. Kim, Alexandra Soboleva, Maxim Tomashevsky, Kimberly A. Marshall, Katherine H. Phillippy, Patti M. Sherman, Rolf N. Muertter, and Ron Edgar. NCBI GEO: Archive for high-throughput functional genomic data. *Nucleic Acids Research*, 37(SUPPL. 1):885–890, 2009. ISSN 03051048. doi: 10.1093/nar/gkn764.
- [56] Adam P. Arkin, Robert W. Cottingham, Christopher S. Henry, Nomi L. Harris, Rick L. Stevens, Sergei Maslov, Paramvir Dehal, Doreen Ware, Fernando Perez, Shane Canon, Michael W. Sneddon, Matthew L. Henderson, William J. Riehl, Dan Murphy-Olson, Stephen Y. Chan, Roy T. Kamimura, Sunita Kumari, Meghan M. Drake, Thomas S. Brettin, Elizabeth M. Glass, Dylan Chivian, Dan Gunter, David J. Weston, Benjamin H. Allen, Jason Baumohl, Aaron A. Best, Ben Bowen, Steven E. Brenner, Christopher C. Bun, John Marc Chandonia, Jer Ming Chia, Ric Colasanti, Neal Conrad, James J. Davis, Brian H. Davison, Matthew DeJongh, Scott Devoid, Emily Dietrich, Inna Dubchak, Janaka N. Edirisinghe, Gang Fang, José P. Faria, Paul M. Frybarger, Wolfgang Gerlach, Mark Gerstein, Annette Greiner, James Gurtowski, Holly L. Haun, Fei He, Rashmi Jain, Marcin P. Joachimiak, Kevin P. Keegan, Shinnosuke Kondo, Vivek Kumar, Miriam L. Land, Folker Meyer, Marissa Mills, Pavel S. Novichkov, Taeyun Oh, Gary J. Olsen, Robert Olson, Bruce Parrello, Shiran Pasternak, Erik Pearson, Sarah S. Poon, Gavin A. Price, Srividya Ramakrishnan, Priya Ranjan, Pamela C. Ronald, Michael C. Schatz, Samuel M.D. Seaver, Maulik Shukla, Roman A. Sutormin, Mustafa H. Syed, James Thomason, Nathan L. Tintle, Daifeng Wang, Fangfang Xia, Hyunseung Yoo, Shinjae Yoo, and Dantong Yu. KBase: The United States department of energy systems biology knowledgebase. *Nature Biotechnology*, 36(7):566–569, 2018. ISSN 15461696. doi: 10.1038/nbt.4163.
- [57] Mark Lotkin. A Note on the Midpoint Method of Integration. *Journal of the ACM (JACM)*, 3(3):208–211, 1956. ISSN 1557735X. doi: 10.1145/320831.320840.
- [58] L. F. Shampine. Stability of the leapfrog/midpoint method. *Applied Mathematics and Computation*, 208(1):293–298, 2009. ISSN 00963003. doi: 10.1016/j.amc.2008.11.029. URL <http://dx.doi.org/10.1016/j.amc.2008.11.029>.
- [59] J. C. Butcher. A history of Runge-Kutta methods. *Applied Numerical Mathematics*, 20:247–260, 1996.
- [60] W. H. Witty. A New Method of Numerical Integration of Differential Equations. *Mathematics of Computation*, 18(87):497, 1964. ISSN 00255718. doi: 10.2307/2003774.
- [61] Ali Ebrahim, Joshua A. Lerman, Bernhard O. Palsson, and Daniel R. Hyduke. COBRAPy: COnstraints-Based Reconstruction and Analysis for Python. *BMC Systems Biology*, 7, 2013. ISSN 17520509. doi: 10.1186/1752-0509-7-74.

- [62] Rosemarie Wilton, Angela J. Ahrendt, Shalaka Shinde, Deirdre J. Sholto-Douglas, Jessica L. Johnson, Melissa B. Brennan, and Kenneth M. Kemner. A New Suite of Plasmid Vectors for Fluorescence-Based Imaging of Root Colonizing Pseudomonads. *Frontiers in Plant Science*, 8(February):1–15, 2018. ISSN 1664462X. doi: 10.3389/fpls.2017.02242.
- [63] Ramy K. Aziz, Daniela Bartels, Aaron Best, Matthew DeJongh, Terrence Disz, Robert A. Edwards, Kevin Formsma, Svetlana Gerdes, Elizabeth M. Glass, Michael Kubal, Folker Meyer, Gary J. Olsen, Robert Olson, Andrei L. Osterman, Ross A. Overbeek, Leslie K. McNeil, Daniel Paarmann, Tobias Paczian, Bruce Parrello, Gordon D. Pusch, Claudia Reich, Rick Stevens, Olga Vassieva, Veronika Vonstein, Andreas Wilke, and Olga Zagnitko. The RAST Server: Rapid annotations using subsystems technology. *BMC Genomics*, 9:1–15, 2008. ISSN 14712164. doi: 10.1186/1471-2164-9-75.
- [64] Christopher S. Henry, Matthew Dejongh, Aaron A. Best, Paul M. Frybarger, Ben Lindsay, and Rick L. Stevens. High-throughput generation, optimization and analysis of genome-scale metabolic models. *Nature Biotechnology*, 28(9):977–982, 2010. ISSN 10870156. doi: 10.1038/nbt.1672.
- [65] Kristian Jensen, Joao G.R. Cardoso, and Nikolaus Sonnenschein. Optlang: An algebraic modeling language for mathematical optimization. *The Journal of Open Source Software*, 2(9):139, 2017. doi: 10.21105/joss.00139.
- [66] S. Lee McGill, Yeni Yung, Kristopher A. Hunt, Michael A. Henson, Luke Hanley, and Ross P. Carlson. *Pseudomonas aeruginosa* reverse diauxie is a multidimensional, optimized, resource utilization strategy. *Scientific Reports*, 11(1):1–16, 2021. ISSN 20452322. doi: 10.1038/s41598-020-80522-8. URL <https://doi.org/10.1038/s41598-020-80522-8>.
- [67] Christopher E. Lawson, William R. Harcombe, Roland Hatzenpichler, Stephen R. Lindemann, Frank E. Löffler, Michelle A. O’Malley, Héctor García Martín, Brian F. Pfleger, Lutgarde Raskin, Ophelia S. Venturelli, David G. Weissbrodt, Daniel R. Noguera, and Katherine D. McMahon. Common principles and best practices for engineering microbiomes. *Nature Reviews Microbiology*, 17(12):725–741, 2019. ISSN 17401534. doi: 10.1038/s41579-019-0255-9. URL <http://dx.doi.org/10.1038/s41579-019-0255-9>.